Circ_0070203 Promotes Epithelial Mesenchymal Transition in Ovarian Serous Cystadenocarcinoma through miR-370-3p/TGFβR2 Axis

Qiong Tang
Southern Medical University
Huiting Wen
Southern Medical University
Xiaoli Chen
Southern Medical University Affiliated Maternal and Children's Hospital of Foshan
Xiushu Xu
Southern Medical University
Xiaoer Chen
Southern Medical University
Yu Fang
Southern Medical University
Yingshan Gao
Southern Medical University
Liu longyang
Nanfang Hospital
Jing Li (lijing7405@126.com)
Nanfang Hospital

Research Article

Keywords: circ_0070203, miR-370-3p,TGFβR2, invasion, metastasis, epithelial mesenchymal transformation,ovarian serous cystadenocarcinoma

Posted Date: November 16th, 2021

DOI: https://doi.org/10.21203/rs.3.rs-1036753/v1

Abstract

Background: Ovarian serous cystadenocarcinoma (OC) is a common malignant gynecological tumor that is found in women. Metastasis of ovarian cancer cells are the main causes of poor prognosis. Cell-acquired invasiveness is accompanied by the loss of epithelial features and gain of a mesenchymal phenotype, through a process known as epithelial–mesenchymal transition (EMT). Circular RNAs (circRNAs) are important biological molecules that are associated with pathogenesis of Multiple cancers; however, the roles of circRNAs and EMT in OC remain unclear.

Methods: Using circRNA microarray, the circRNA expression profiles in ovarian tissues, with and without OC, were identified and verified using quantitative reverse transcription PCR (RT-qPCR). The effects of circ_0070203, miR-370-3p, and TGFβR2 on SKOV-3 cell migration and invasion were evaluated. The binding sites between circ_0070203, miR-370-3p, and TGFβR2 were verified by dual-luciferase reporter assay and bioinformatics analysis. The expression levels of epithelial mesenchymal transformation-related proteins were detected by western blotting. Cell migration and invasion were analyzed by a transwell assay.

Results: Circ_0070203 and TGFβR2 were upregulated, while miR-370-3p was downregulated in OC and SKOV-3 cell lines. The overexpression of circ_0070203 changed the expression of other EMT-related proteins, and enhanced the invasion and migration abilities of ovarian cancer cells. The inhibitory effect of circ_0070203 knockdown on EMT, migration, and invasion of ovarian cancer cells was partly attenuated by an miR-370-3p inhibitor.

Conclusion: Circ_0070203 promotes epithelial mesenchymal transformation, invasion, and metastasis of ovarian cancer cells via the miR-370-3p /TGFβR2 axis.

Background

Ovarian cancer, with complex molecular pathogenesis and genetic variability, has become a major health concern that seriously threatens the lives and quality of life of women worldwide [1, 2]. Metastasis, especially multi-organ metastasis, is the main cause of ovarian cancer[3, 4]. Studies have shown that epithelial mesenchymal transformation (EMT) imparts the ability of cancer cells to proliferate, invade, and metastasize, thus accelerating the progression of cancer[5–7], including ovarian cancer[8, 9]. Due to the lack of effective prognostic markers, most patients are diagnosed at an advanced stage, and have a poor prognosis. Therefore, exploring the molecular mechanism of metastasis in ovarian cancer and identifying markers for early diagnosis, as well as novel therapeutic targets, is a major area of focus in the field of ovarian cancer research.

Circular RNAs (circRNAs) are associated with tumor progression in liver cancer[10], gastric cancer[11] and esophageal cancer[12]. In addition, Lin et al. found that different-expression levels of circRNAs are associated with invasion, metastasis, and poor prognosis of ovarian cancer[13–15]. Liu et al. found that

circRNAs are involved in the EMT in a variety of indications[16, 17], including ovarian cancer[18, 19]; however, circ_0070203, a newly screened circRNA with unknown function in ovarian cancer tissues, has not been reported in cancer-related studies. Therefore, this study investigates the role of circ_0070203 in the pathogenesis of ovarian serous carcinoma (OC).

We found the upregulation of circ_0070203 expression in ovarian cancer tissues, and verified its presence in the ovarian cancer cell line SKOV-3. Bioinformatics analysis revealed that miR-370-3p shared a common binding site with circ_0070203, and the downstream target protein TGFβR2 was changed correspondingly. Interestingly, we found that the upregulation of circ_0070203, the expression of E-cadherin and SMAD4 decreased, while the expression of N-cadherin, SNAll, and vimentin increased, implying that epithelial mesenchymal transformation occurred, the malignancy of the tumor cells increased. Thus, circ_0070203 promotes ovarian cancer progression through SMAD2 and the SMAD3 /PKA pathway.

In our study, we concluded that circ_0070203 regulates the expression of TGFβR2, through competitive binding with miR-370-3p, and promotes the epithelial mesenchymal transformation, invasion, and metastasis of ovarian cancer cells through the SMAD2/SMAD3/PKA pathway.

Results

Identification of differentially expressed circRNAs in ovarian cancer

To identify differentially expressed genes between OC and normal ovarian cells, gene cluster analysis was performed. Cluster analysis showed that 34 circRNAs in ovarian cancer exhibited expression levels that differed by more than 2.5 times the levels observed in normal tissues ($P<0.05$); 11 circRNAs were upregulated and 23 circRNAs were downregulated,. Moreover, GO and pathway analysis showed that the differentially expressed genes were functionally related to cell processes and regulation, mitotic cycle, ribosome synthesis, DNA replication and transport, invasion, and metastasis, as well as being involved in cell cycle regulation and AMPK signaling pathways (Figure 1). Bioinformatics analysis showed that circ_0070203 was located on the *BMP2K* in the long arm (short arm) of chromosome 4, formed by the cyclization of the exons of the *BMP2K* (Figure 2A). RT-qPCR showed that the expression of circ_0070203 in ovarian cancer tissue was significantly higher than that in normal ovarian tissue ($P = 0.001$), exhibiting the greatest difference the two tissue types and the best uniformity (Figure 2B). In addition, circ_0070203 ($P = 0.046$) was significantly overexpressed in SKOV-3 cells, in comparison to OVCAR3 cells (Figure 2C), thus we chose SKOV-3 cells for subsequent experiments.

Circ_0070203 promotes ovarian cancer progression through epithelial mesenchymal transformation, invasion,

and metastasis of ovarian cancer cells.

After verifying the overexpression of circ_0070203, the expression levels of several proteins related to cancer progression were evaluated. Specifically, SMAD2/3, PAK, PKC, SNAIl, N-cadherin, vimentin, MMP-2, and MMP-9 were found to be significantly increased, while the expression levels of SMAD4 and E-cadherin was significantly decreased in ovarian cancer cell lines. (Figure 3A). Transwell and scratch assays revealed that the number of cells that migrated to, or invaded, the bottom chamber of SKOV-3 cells increased significantly (P<0.0001; P<0.0001) after overexpression of circ_0070203, but decreased (P<0.0001; P<0.0001) significantly after knockdown of circ_0070203 (Figure 3B).

Circ_0070203 directly sponges miR-370-3p in ovarian cancer cells

Bioinformatics analysis indicated binding sites between miR-370-3p and TGFβR2 (Figure 4A).We measured the expression level of miR-370-3p in ovarian cancer tissues by RT-qPCR and found that the expression level of miR-370-3p was significantly lower (P = 0.024) in ovarian cancer tissues, than in normal tissues (Figure 4B). Moreover, miR-370-3p expression was significantly lower (P = 0.015) in SKOV-3 cells than in OVCAR3 cells (Figure 4C). We knocked down or overexpressed circ_ 0070203 in SKOV-3 cells and verified by RT-qPCR, that miR-370-3p expression was decreased (P = 0.025) after overexpression of circ_0070203, and increased (P = 0.003) after knockdown of circ_0070203 (Figure 4D, Figure 3E).

Circ_0070203 regulates TGFβR2 through competitive binding of miR-370-3p,affecting EMT, invasion, and metastasis of ovarian cancer cells.

Bioinformatics indicated binding sites between miR-370-3p and TGFβR2 (Figure 5A). RT-qPCR analysis revealed that the expression of TGFβR2 in ovarian cancer tissue was significantly higher (P = 0.001) than that in normal ovarian tissue (Figure 5B), and TGFβR2 was significantly overexpressed (P = 0.005) in SKOV-3 cells, in comparison to OVCAR3 cells (Figure 5C). We knocked down or overexpressed circ_0070203 in SKOV-3 cells, and via RT-qPCR verified that TGFβR2 expression was increased (P = 0.046) upon overexpression of circ_0070203, and decreased (P = 0.001) after knockdown of circ_0070203 (Figure 5D). Moreover, western blotting confirmed this trend(Figures 5E and 5F. After TGFβR2 overexpression, the expression levels of Smad2/3, PAK, PKC, SNAIl, N-cadherin, vimentin, MMP-2, and MMP-9 were significantly increased, and the expression of SMAD4 and E-cadherin was significantly decreased (Figure 3A). We found that the number of cells that migrated to, or invaded the bottom chamber was higher (P<0.0001; P<0.0001) in the TGFβR2 overexpression group, in comparison to the TGFβR2 knockdown group (Figure 5G).

Binding sites of circ_0070203, miR-370-3p, and TGFβR2

In the experiment of transfection with the 3' UTR of the circ_0070203 plasmid, the dual luciferase activity assay results showed that the relative luciferase activity was lower (P = 0.001; 0.017) after transfection with an miR-370-3p mimic, in comparison to the blank and NC groups, while relative luciferase activity was higher (P = 0.007; 0.010) after miR-370-3p inhibitor transfection, in comparison to miR-NC inhibitor transfection and the blank group (Figure 6A). In the experiments involving transfection with the 3' UTR of mutant circ_0070203 plasmid, there was no significant difference (P = 0.756; 0.924) observed between the miR-370-3p, blank, or NC groups (Figure 6B). In the experiment involving transfection with the 3' UTR of the TGFβR2 plasmid, the relative luciferase activity was lower (P = 0.001; 0.004) after miR-370-3p mimic transfection, in comparison to the blank and NC groups, while relative luciferase activity was higher (P = 0.002; 0.004) after miR-370-3p inhibitor transfection, in comparison to miR-NC inhibitor transfection, and the blank group (Figure 6C). In the experiment involving transfection with the 3' UTR of mut no. 1 TGFβR2 plasmid, the relative luciferase activity was lower (P = 0.0004) after miR-370-3p mimic transfection, in comparison to the NC group (Figure 6D). Furthermore, in the experiment involving transfection with the 3' UTR of mut no. 2 TGFβR2 plasmid, the relative luciferase activity was lower (P = 0.004; 0.001) after miR-370-3p mimic transfection, in comparison to the blank and NC groups (Figure 6E). Finally, in the experiment involving transfection with the 3' UTR of mut 2 sites TGFβR2 plasmid, there was no significant difference (P = 0.618 ; 0.067) between the miR-370-3p, blank, and NC groups (Figure 6F).

Inhibitory effect of circ_0070203 knockdown on ovarian cancer cell EMT, migration, and invasion was partly attenuated by miR-370-3p inhibitor

We found that TGFβR2 expression increased (P = 0.001) after circ_0070203 knockdown and mir-370-3p silencing, simultaneously (Figure 7A). Moreover, the expression levels of TGFβR2, SMAD2/3, PAK, PKC, SNAIl, N-cadherin, vimentin, MMP-2, and MMP-9 were significantly increased, while the expression of SMAD4 and E-cadherin was significantly decreased, under the same conditions of simultaneous circ_0070203 knockdown and mir-370-3p silencing (Figure 7B). We found that the number of cells that migrated to, or invaded the bottom chamber increased significantly (P = 0.018; P <0.0001) after simultaneous circ_0070203 knockdown and miR-370-3p silencing (Figure 7C).

Discussion

Invasion and metastasis are one of the main characteristics of malignant tumors; however, EMT of tumor cells is the key to tumor metastasis. EMT activation leads to a decrease in E-cadherin, and an increase in N-cadherin, vimentin, MMPs, and other molecules, as well as a decrease in intercellular adhesion, and the malignant degree of cancer cells, which promotes the invasion and metastasis of tumor cells[5, 6, 8]. OC is a common tumor with poor prognosis in women, which lacks effective prevention and treatment. Although there have been several studies that have focused on the identifying of markers of ovarian cancer, our understanding of its progression remains at a fairly immature stage[20, 21].

In recent years, an increasing number of studies have found that circRNAs are associated with EMT and the progression of ovarian cancer[22, 23]. In our study, we found that circ_0070203 was overexpressed in ovarian serous cystadenocarcinoma, and confirmed that circ_0070203 can promote the EMT, invasion, and metastasis of ovarian cancer cells in vitro, indicating that circ_0070203 is intimately involved in the malignant progression of ovarian cancer.

Studies have shown that circRNAs and miRNAs play an irreplaceable role in progression. Memczak and Kosik et al. found that circRNAs can act as a "sponge" to absorb miRNA and act as competitive endogenous RNA (ceRNA), changing the level of miRNA target genes, thus affecting the carcinogenic and cancer suppressive ability of miRNA[24, 25]. Wang Z et al. found that circ-03955 promotes EMT in osteosarcoma by competitively sponging miR-3662[26]. In our study, we found that both circ_0070203 and TGFβR2 have miR-370-3p binding sites, by bioinformatics analysis, and verified this using a dual-luciferase reporter assay.

It has been reported that TGFβR2 can promote tumor progression and is one of the target genes of miR-370-3p.[27] Through cell experiments and tissue validation, we found that circ_0070203 expression was negatively correlated with miR-370-3p, and positively correlated with TGFβR2. Transwell assay also confirmed that high expression of circ_0070203 and TGFβR2 could promote EMT, invasion, and metastasis of ovarian cancer cells. Additionally, rescue experiments demonstrated that miR-370-3p inhibition rescued the inhibitory effects on EMT, invasion, and metastasis of ovarian cancer cells via circ_0070203 knockdown.

In this study, we have revealed the role of circ_0070203 and miR-370-3p in inducing EMT in SKOV-3 cells. We also demonstrated the relationship between circ_0070203 and miR-370-3p. Moreover, circ_0070203 decreased the expression of the E-cadherin and upregulated the morphology, SNAIl and vimentin, promoting EMT in cancer cells. Our results indicate that the circ_0070203–miR-370-3p–TGFβR2 axis is a possible molecular target for the prevention of EMT in human ovarian cancer.

Based upon previous research, we have strived to be innovative in our approach to determining the molecular mechanism involved in ovarian cancer invasion and metastasis, and to identify targets and predictive indicators for the treatment of ovarian cancer.

Conclusions

In conclusion, circ_0070203 expression was significantly upregulated in ovarian cancer tissues. Furthermore, circ_0070203 promoted ovarian cancer cell migration and invasion. Taken together, our results verify that circ_0070203 acts as a ceRNA to sponge miR-370-3p off and regulate the expression of TGFβR2, thus participating in the regulation of the TGF-β/SMAD signaling EMT to further accelerate invasion and metastasis of ovarian cancer cells. Circ_0070203 plays a significant role in promoting the malignant progression of ovarian cancer, so it is expected to be a marker for predicting ovarian cancer.

Methods

Ovarian tissues

12 cases of OC and normal ovarian tissues respectively, diagnosed in the pathology department of Nanfang Hospital of Southern Medical University in Guangzhou province of China from January 2020 to January 2021, were collected and used in this study.

CircRNA Microarray Analysis

The differential expression of circRNAs in three pairs of ovarian cancer tissues and normal ovarian tissues were detected using the Human circular microarray co-expression chip.

RT-qPCR

PCR primers were designed, and their sequences are listed in Table 1. Total cell RNA was extracted using Trizol reagent, according to the Thermo Fisher Scientific manufacturer's instructions, and the concentration and purity of RNA were detected using a UV-vis spectrophotometer. The total RNA was reverse transcribed, and detected using SYBR Green PCR. Ct values obtained by qPCR were calculated using the $2^{-\Delta\Delta Ct}$ method.β-actin served as the internal control.

Table 1

Primer sequences used for qRT-PCR

Primer name	Sequence (5'–3')
circ_0070203-F	AGTGGTGACATAAAAGGGCTG
circ_0070203-R	GCTTCACTAGCAGTCATCGG
TGFβR2-F	TGGTGTGTGAGACGTTGACT
TGFβR2-R	AAGGCATGCTGACGACTCTGTG
miR-370-F	AAGGCATGCTGACGACTCTGTG
miR-370-R	AGCTCACTCACATAGATGAGAG
β-actin-F	GCATGGGTCAGAAGGATTCCT
β-actin-R	TCGTCCCAGTTGGTGACGAT
U6-F	CTCGCTTCGGCAGCACA
U6-R	AACGCTTCACGAATTTGCGT
U6-RT	AACGCTTCACGAATTTGCGT
Abbreviations: F, forward primer; qRT-PCR, quantitative reverse-transcription PCR; R, reverse primer.	

Bioinformatic Analysis

Detailed information on circ_0070203 was obtained from circBase (http://www.circbase.org/). Target microRNAs (miRNAs) of circ_0070203 were predicted using the Circular RNA Interactome (https://circinteractome.nia.nih.gov/

) . The target mRNAs of miR-370-3p were predicted using miRDB (http://mirdb.org/miRDB/) , TargetScan (http://targetscan.org).

Cell culture and transfection

SKOV-3 and OVCAR3 cells were cultured in RPMI 1640 medium with 10% FBS at 37 °C and 5% CO_2. The full length circ_0070203, miR-370-3p, and TGFβR2 were synthesized, and the siRNA sequences of circ_0070203, miR-370-3p, and TGFβR2 were designed using the siRNA online design software. The associated siRNA molecules were linked to lentivirus vectors. Stable cell lines were screened to determine whether circ_0070203, miR-370-3p, and TGFβR2 were successfully overexpressed and interfered with.

Dual Luciferase reporter Assay

Cells were co-transfected with a recombinant luciferase reporter plasmid containing the wild-type or mutant circ_0070203 sequence, along with wild-type or mutant TGFβR2 sequence. The renilla and firefly luciferase activity was measured using a Promega GloMax96 microplate luminescence detector after transfection for 48 h, according to the manufacturer's instructions. Relative luciferase activity was calculated using the ratio of luciferase activity (R/F) of renilla and firefly. Primers used for the luciferase reporter assay are shown in Table 2.

Table 2

Primers for luciferase reporter assay

Primer name	Sequence (5'–3')
circ_0070203-XhoIF	ccgctcgagAATTCTTCTATTCCTTCAGCTCTTCCT
circ_0070203-NotIR	ataagaatgcggccgcTCTGATTTAAAGTGAAAAAGAATTTATTTA
Mut circ_0070203-F	CCAGCAACTATCATCAAGAGATTGGAGATTACAGCAACTCCATTTACAGCATCG
Mut circ_0070203-R	GTAATCTCCAATCTCTTGATGATAGTTGCTGGAGTACTCTATGCTGCTGTGGCG
TGFβR2-XhoIF	ccgctcgagCTCTTCTGGGGCAGGCTGGGCCATGTCCAA
TGFβR2-NotIR	ataagaatgcggccgcTTTAGCTACTAGGAATGGGAACAGGA
Mut TGFβR2-1F	AAGAACAGAGGTCATCAACAGCTGCCCCTGAACTGATGCTTCCTGGAAAACCAA
Mut TGFβR2-1R	GGGGCAGCTGTTGATGACCTCTGTTCTTTGGTGAGAGGGGCAGCCTCTTTGGAC
Mut TGFβR2-2F	GCAGAAACAACAGTCATCAAGAGTGGGTGACATAGAGCATTCTATGCCTTTGAC
Mut TGFβR2-2R	GTCACCCACTCTTGATGACTGTTGTTTCTGCTTATCCCCACAGCTTACAGGGAG
Abbreviations: F, forward primer ;R, reverse primer.	

Cell Migration and Invasion Assay

Cells at the logarithmic-growth stage were washed with fetal bovine serum supplemented RMI 1640 medium, and cell suspensions were prepared. A 200 μL cell suspension aliquot was added into the upper chamber of the transwell chamber. A 600 μL aliquot of RPMI 1640 media supplemented with 10% fetal bovine serum was added into the lower chamber and cultured for 24 h. Transwell chambers were removed and cleaned twice with PBS. Residual cells were wiped with a cotton swab, and the transmembrane cells were stained with crystal violet and counted to represent the number of migrating

cells. Matrigel glue was laid on top of polycarbonate film in Transwell chamber. Cell invasion was evaluated and represented by the number of cells passing through the Matrigel gel.

Western Blot Analysis

Tissue samples were collected and lysed with RIPA lysis buffer (Beyotime Biotechnology) to extract total protein content. Protein concentration was quantified with a bicinchoninic acid protein assay kit (Beyotime Biotechnology). According to the principal sample of total protein consistency, 10% of the separated gel was subjected to SDS-PAGE electrophoresis. After being transferred at 100 V for 50 min, the membranes were incubated with 5% skim milk powder at 37 °C for 1 h; followed by washing thrice with TBST for ten minutes, and were incubated overnight with the following primary antibodies at 4°C: TGFβR2 (1:1000; Abcam), anti-E-cadherin (1:1000; Abcam), anti-Smad2/3 (1:1000; Abcam), anti-Smad4 (1:1000; Abcam), anti-N-cadherin (1:5000; Abcam)and anti-Snail (1:1000; Abcam), anti-MM2 (1:1000; Abcam), anti-MM9 (1:1000; Abcam), anti-PAK (1:1000; Abcam), anti- PKC (1:1000; Abcam), (1:1000; Abcam) or anti-vimentin (1:1000; Abcam). The membrane was washed with TBST three times for 10 min, followed by incubation with the following secondary antibodies:Goat Anti-Rabbit IgG(H+L) (1:10000;southern biotech), Rabbit Anti-Mouse IgG(H+L)-HRP (1:20000;southern biotech) respectively at room temperature for 1 h. Finally, the membranes were washed with TBST three times for 10 min and were imaged. The densitometric analysis was carried out using the Image Pro-Plus 6.0 software (Media Cybernetics, Silver Spring, MD, USA).

Statistical Analysis

Statistical analysis was performed using the SPSS (version 26.0; IBM, Armonk, NY, USA) and GraphPad Prism (version 8.0; GraphPad Software, San Diego, CA, USA) software. Data are expressed as mean ± standard deviation (SD). The unpaired *t*-test was used when the data were normally distributed, and the nonparametric test was used when the data were not normally distributed. tatistical significance was set at $P < 0.05$.

Abbreviations

OC: Ovarian serous cystadenocarcinoma;

EMT: epithelial–mesenchymal transition;

circRNAs: Circular RNAs;

miRNAs: microRNAs;

TGFβR2: Transforming Growth Factor-beta Receptor type II

Declarations

Ethics approval and consent to participate

The use of patients' tissues and data for the study had obtained written consents from all participates. The study was approved by The Ethics Committee of the Nanfang Hospital, Southern Medical University with the following reference number: NO. LW2018001, and the research were conducted in conformity with the Declaration of Helsinki and the NIH guidelines (NIH Pub. No. 85–23, revised 1996).

Consent for publication

Not Applicable

Availability of data and material

The websites of the databases as mentioned above are open. The datasets used and/or analyzed during the current study available from the corresponding author on reasonable request.

Competing interests

The authors report no conflicts of interest in this work.

Funding

This study was supported by Guangdong Province Natural Science Foundation of China (No.2021A1515011845). The funding bodies fund experimental materials and paper publication, but had no involvement in the design of the study, collection, analysis, and interpretation of data and in writing the manuscript.

Authors' contributions

QT and HTW contributed equally to this article. JL and LYL designed the experiment. QT and HTW and XLC performed the experiments and analyzed the data. SXX, XEC, FY and YSG participated in the performance of the experiments and collection of the tissues. QT wrote the manuscript. All authors read and approved the final manuscript.

Acknowledgements

We thank professor JL for valuable comments during the study implementation.

References

1. Hennessy B T, Coleman R L, Markman M. Ovarian cancer[J]. Lancet, 2009,374(9698):1371–1382.
2. Bowtell D D. The genesis and evolution of high-grade serous ovarian cancer[J]. Nat Rev Cancer, 2010,10(11):803–808.
3. Kebapcı E, Gülseren V, Tuğmen C, et al. Outcomes of patients with advanced stage ovarian cancer with intestinal metastasis[J]. Ginekol Pol, 2017,88(10):537–542.
4. Gloss B S, Samimi G. Epigenetic biomarkers in epithelial ovarian cancer[J]. Cancer Lett, 2014,342(2):257–263.
5. Lamouille S, Xu J, Derynck R. Molecular mechanisms of epithelial-mesenchymal transition[J]. Nat Rev Mol Cell Biol, 2014,15(3):178–196.
6. Dongre A, Weinberg R A. New insights into the mechanisms of epithelial-mesenchymal transition and implications for cancer[J]. Nat Rev Mol Cell Biol, 2019,20(2):69–84.
7. Xu Q, Deng F, Qin Y, et al. Long non-coding RNA regulation of epithelial-mesenchymal transition in cancer metastasis[J]. Cell Death Dis, 2016,7(6):e2254.
8. Liu L, Wu N, Wang Y, et al. TRPM7 promotes the epithelial-mesenchymal transition in ovarian cancer through the calcium-related PI3K / AKT oncogenic signaling[J]. J Exp Clin Cancer Res, 2019,38(1):106.
9. Liang H, Yu T, Han Y, et al. LncRNA PTAR promotes EMT and invasion-metastasis in serous ovarian cancer by competitively binding miR-101-3p to regulate ZEB1 expression[J]. Mol Cancer, 2018,17(1):119.
10. Wang X, Wang X, Li W, et al. Up-Regulation of hsa_circ_0000517 Predicts Adverse Prognosis of Hepatocellular Carcinoma[J]. Front Oncol, 2019,9:1105.
11. Huang M, He Y R, Liang L C, et al. Circular RNA hsa_circ_0000745 may serve as a diagnostic marker for gastric cancer[J]. World J Gastroenterol, 2017,23(34):6330–6338.
12. Fan L, Cao Q, Liu J, et al. Circular RNA profiling and its potential for esophageal squamous cell cancer diagnosis and prognosis[J]. Mol Cancer, 2019,18(1):16.
13. Lin C, Xu X, Yang Q, et al. Circular RNA ITCH suppresses proliferation, invasion, and glycolysis of ovarian cancer cells by up-regulating CDH1 via sponging miR-106a[J]. Cancer Cell Int, 2020,20:336.
14. Zhao Y, Hu Y, Shen Q, et al. CircRNA_MYLK promotes malignant progression of ovarian cancer through regulating microRNA-652[J]. Eur Rev Med Pharmacol Sci, 2020,24(10):5281–5291.
15. Zhang C, Liu W, Li F, et al. Hsa_circ_0015326 Promotes the Proliferation, Invasion and Migration of Ovarian Cancer Through miR-127-3p/MYB[J]. Cancer Manag Res, 2021,13:2265–2277.
16. Wang L, Tong X, Zhou Z, et al. Circular RNA hsa_circ_0008305 (circPTK2) inhibits TGF-β-induced epithelial-mesenchymal transition and metastasis by controlling TIF1γ in non-small cell lung cancer[J]. Mol Cancer, 2018,17(1):140.

17. Shang B Q, Li M L, Quan H Y, et al. Functional roles of circular RNAs during epithelial-to-mesenchymal transition[J]. Mol Cancer, 2019,18(1):138.
18. Li X, Lin S, Mo Z, et al. CircRNA_100395 inhibits cell proliferation and metastasis in ovarian cancer via regulating miR-1228/p53/epithelial-mesenchymal transition (EMT) axis[J]. J Cancer, 2020,11(3):599–609.
19. Wang W, Zhang W, Guo H, et al. CircLNPEP promotes the progression of ovarian cancer through regulating miR-876-3p/ WNT5A axis[J]. Cell Cycle, 2021:1–19.
20. Grunewald T, Ledermann J A. Targeted Therapies for Ovarian Cancer[J]. Best Pract Res Clin Obstet Gynaecol, 2017,41:139–152.
21. Pan C, Stevic I, Müller V, et al. Exosomal microRNAs as tumor markers in epithelial ovarian cancer[J]. Mol Oncol, 2018,12(11):1935–1948.
22. Ding J, Wang Q, Guo N, et al. CircRNA circ_0072995 promotes the progression of epithelial ovarian cancer by modulating miR-147a/CDK6 axis[J]. Aging (Albany NY), 2020,12(17):17209–17223.
23. Zeng X Y, Yuan J, Wang C, et al. circCELSR1 facilitates ovarian cancer proliferation and metastasis by sponging miR-598 to activate BRD4 signals[J]. Mol Med, 2020,26(1):70.
24. Memczak S, Jens M, Elefsinioti A, et al. Circular RNAs are a large class of animal RNAs with regulatory potency[J]. Nature, 2013,495(7441):333–338.
25. Kosik K S. Molecular biology: Circles reshape the RNA world[J]. Nature, 2013,495(7441):322–324.
26. Wang Z, Deng M, Chen L, et al. Circular RNA Circ-03955 Promotes Epithelial-Mesenchymal Transition in Osteosarcoma by Regulating miR-3662/Metadherin Pathway[J]. Front Oncol, 2020,10:545460.
27. Zhang S, Song G, Yuan J, et al. Circular RNA circ_0003204 inhibits proliferation, migration and tube formation of endothelial cell in atherosclerosis via miR-370-3p/TGFβR2/phosph-SMAD3 axis[J]. J Biomed Sci, 2020,27(1):11.

Figures

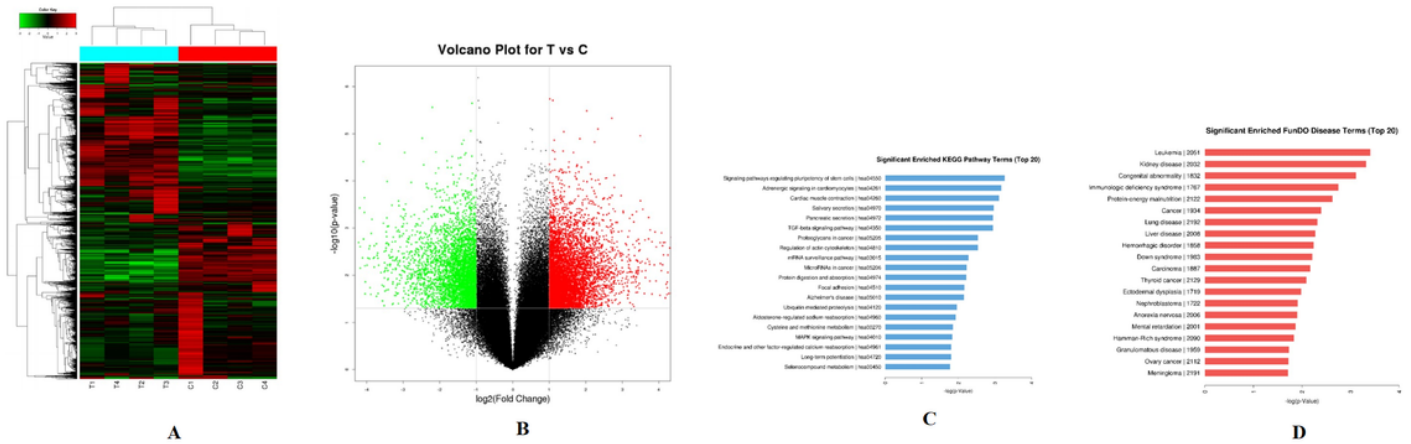

Figure 1

(A) cluster analysis of circRNA microarray results; (B) circRNA tissue microarray results suggested the volcanic map of ovarian cancer tissue expression level, in comparison with normal ovarian tissue; (C) KEGG pathway analysis of circRNA tissue microarray;(D) GO analysis of circRNA tissue microarray.

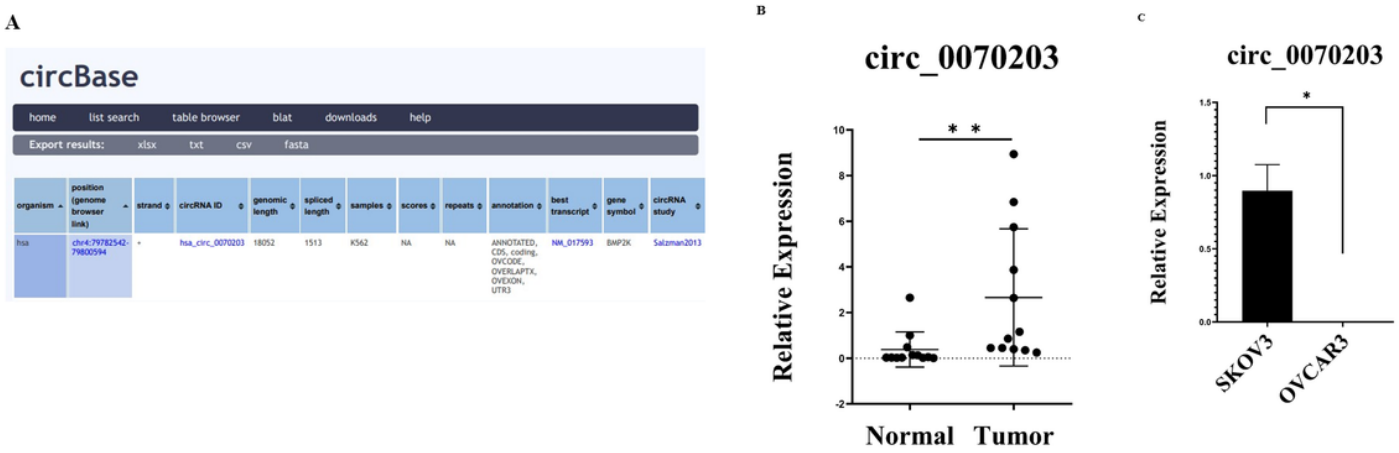

Figure 2

(A) Bioinformatics information of circ_0070203; (B)Expression levels of circ_0070203 in ovarian cancer tissue and normal ovarian tissue; (C)Expression levels of circ_0070203 in SKOV-3 and OVCAR3 cells. *P<0.05

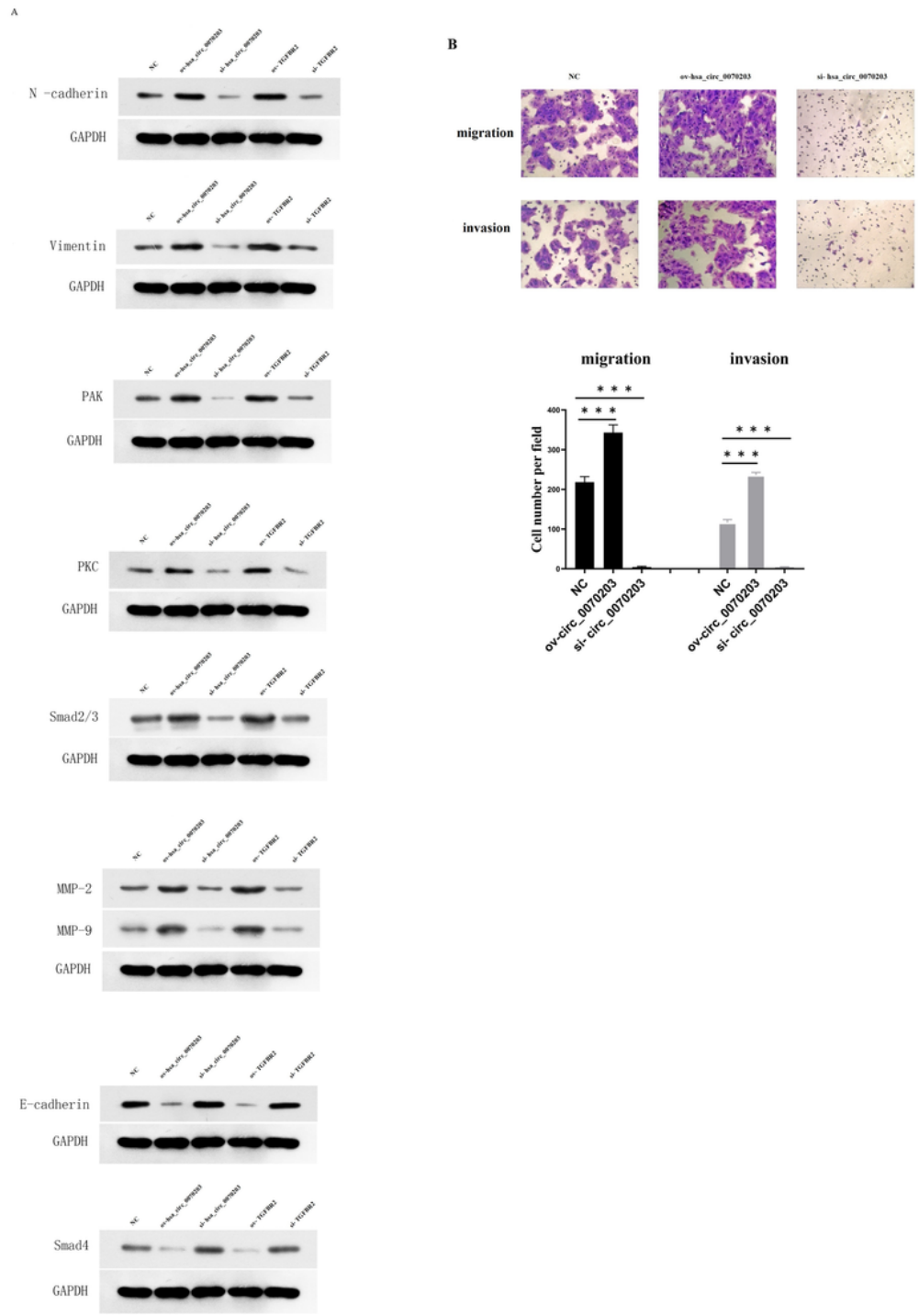

Figure 3

(A) Expression levels of Smad2/3, PAK, PKC, SNAIl, N-cadherin, Vimentin, MMP-2, MMP-9, Smad4, and e-cadherin in the cells of overexpression circ_0070203, the cells of knockdown circ_0070203, the cells of overexpression TGFβR2 and the cells of knockdown TGFβR2 were measured by western bolt; (B) Expression levels of SMAD4 and E-cadherin the cells engineered to overexpress circ_0070203, and cells

where circ_0070203 is knocked down; (C) Migration and invasion of ovarian cancer cells SKOV-3 after silencing and overexpressing circ_0070203, by Transwell assay and scratch assay.

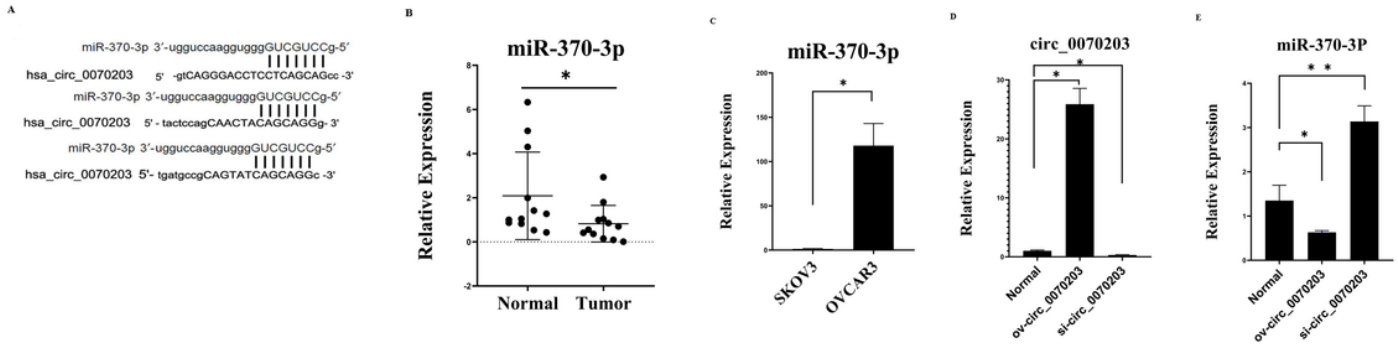

Figure 4

(A) Binding site of circ_0070203 and miR-370-3p; (B) Expression levels of miR-370-3p in ovarian cancer tissue and normal ovarian tissue, measured by RT-qPCR assay; (C) Expression levels of miR-370-3p in SKOV-3 cells and OVCAR3, measured by RT-qPCR assay; (D) Expression levels of circ_0070203 in cells overexpressing circ_0070203, and cells where circ_0070203 is knocked down, measured by RT-qPCR assay; (E) Expression levels of miR-370-3p in the cells overexpressing circ_0070203, and cells where circ_0070203 is knocked down, measured by RT-qPCR assay.

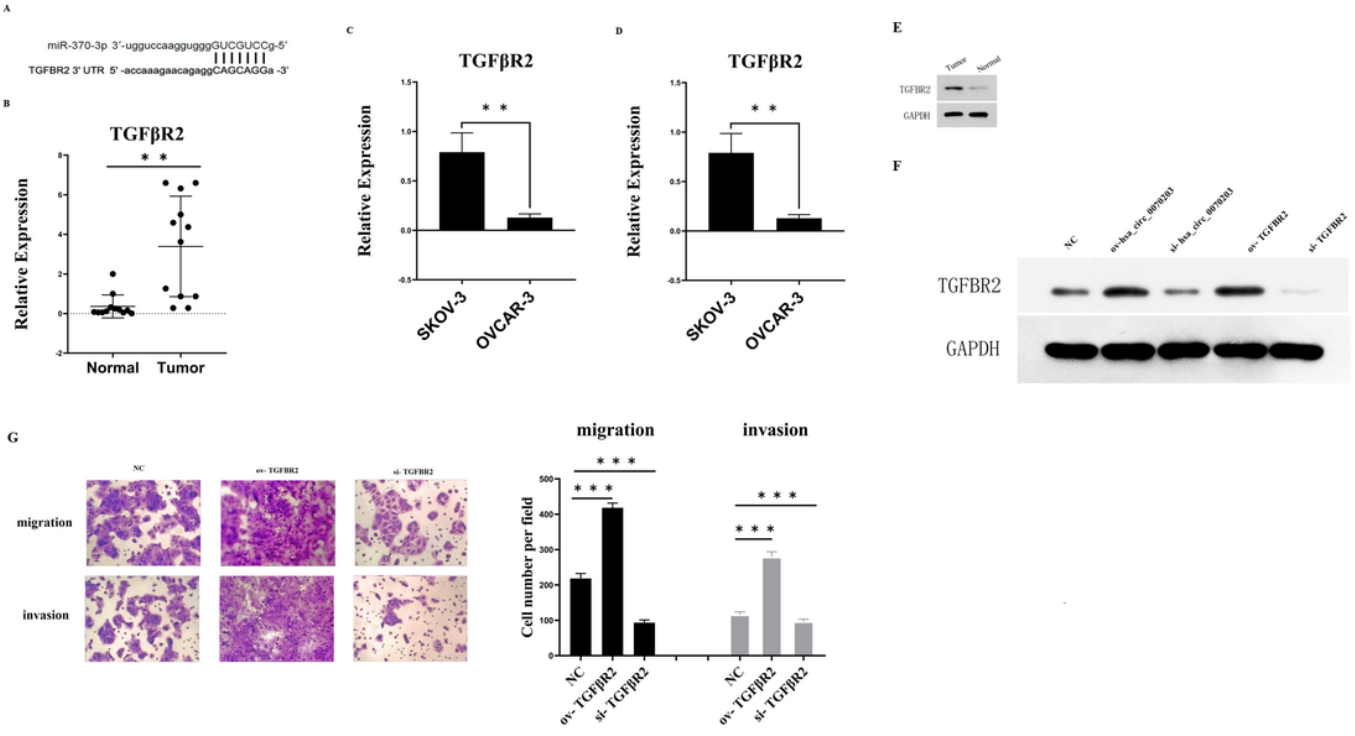

Figure 5

(A) Binding site between miR-370-3p and TGFβR2; (B) Expression levels of TGFβR2 in ovarian cancer tissue and normal ovarian tissue, measured by RT-qPCR assay; (C) Expression levels of TGFβR2 in SKOV-3 cells and OVCAR3, measured by RT-qPCR assay; (D) Expression levels of TGFβR2 in the cells overexpressing circ_0070203, and cells where circ_0070203 is knocked down, measured by RT-qPCR assay; (E) Expression levels of TGFβR2 in SKOV-3 cells and OVCAR3 were measured by western blot; (F) Expression levels of TGFβR2 in cells overexpressing circ_0070203, and cells where circ_0070203 is knocked down, measured by western blot; (G) Migration and invasion of ovarian cancer cells SKOV-3 after silencing and overexpressing TGFβR2 by Transwell and scratch assays.

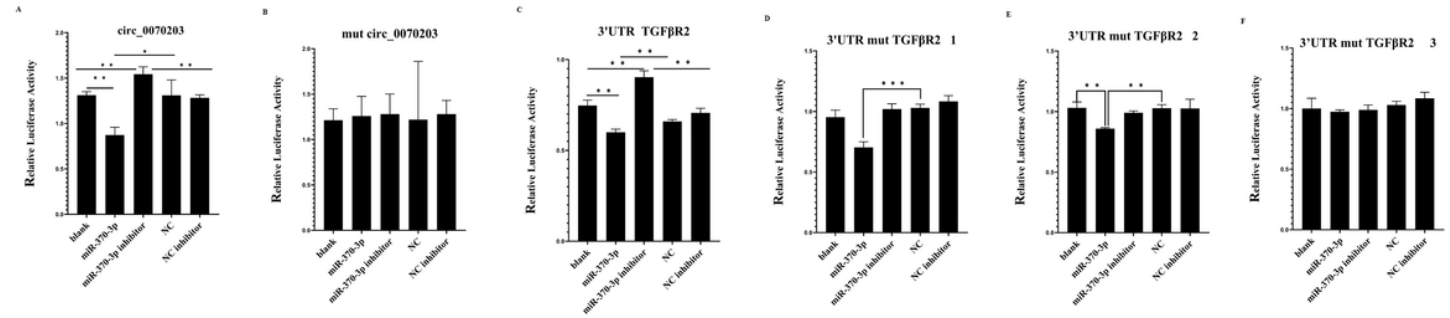

Figure 6

(A) Results of the dual luciferase activity assay in transfection with the 3' UTR of the circ_0070203 plasmid; (B) Results of the dual luciferase activity assay in transfection with the 3' UTR of the mut circ_0070203 plasmid; (C) Results of the dual luciferase activity assay in transfection with the 3' UTR of the TGFβR2 plasmid; (D) Results of the dual luciferase activity assay in transfection with the 3' UTR of the mut no. 1 TGFβR2 plasmid; (E) Results of the dual luciferase activity assay in transfection with the 3' UTR of the mut no. 2 TGFβR2 plasmid; (F) Results of the dual luciferase activity assay in transfection with the 3' UTR of the mut no. 1 and the no. 2 TGFβR2 plasmid.

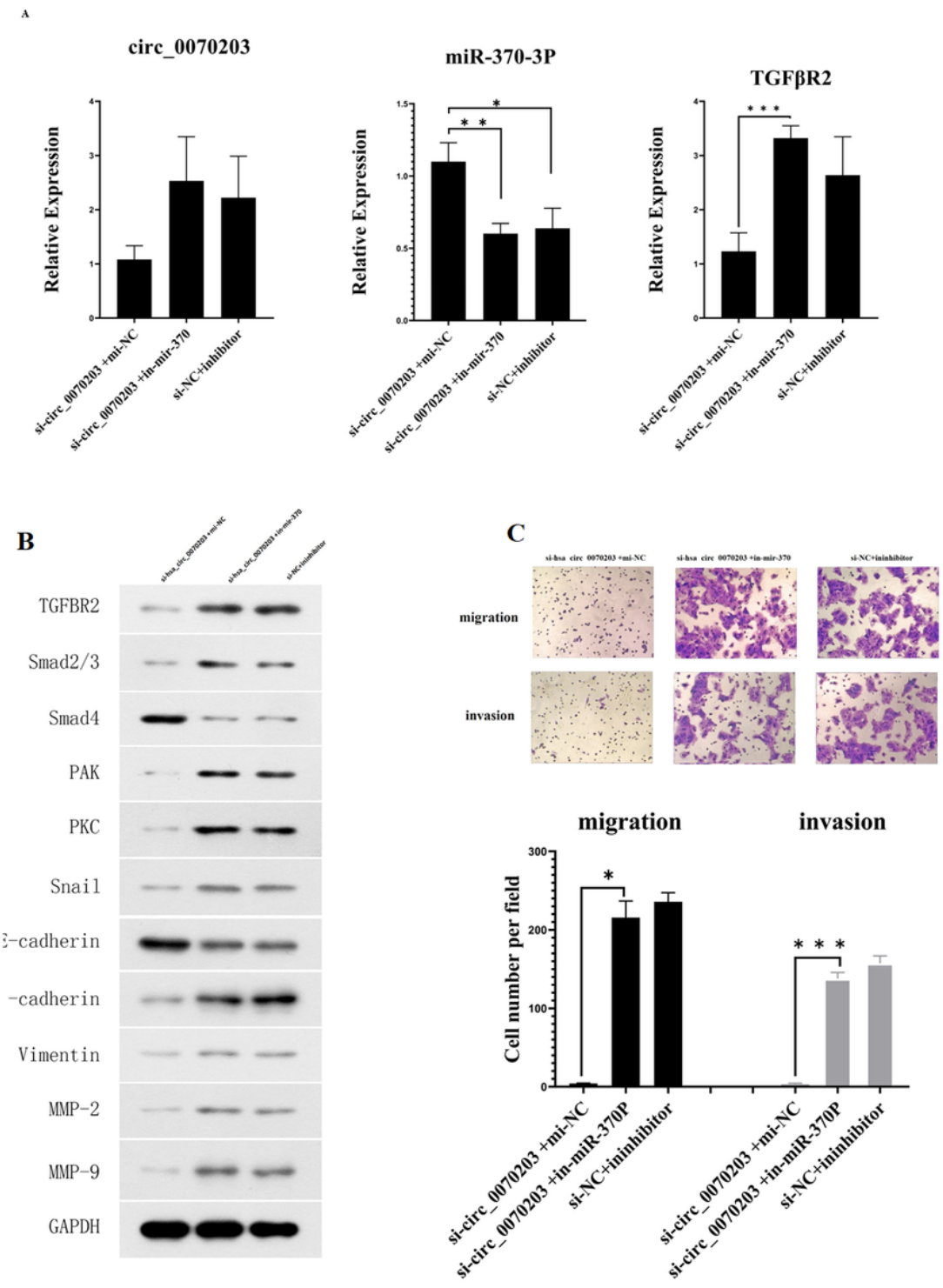

Figure 7

(A) Expression levels of TGFβR2, circ_0070203, and miR-370-3p in cells with simultaneous circ_0070203 knockdown and miR-370-3p silencing, measured by RT-qPCR assay; (B) Expression levels of TGFβR2, SMAD2/3, PAK, PKC, SNAI1, N-cadherin, Vimentin, MMP-2, MMP-9, SMAD4 and E-cadherin the cells with simultaneous circ_0070203 knockdown and miR-370-3p silencing, measured by western blot; (C)

Migration and invasion of ovarian cancer cells SKOV-3 after simultaneously silencing circ_0070203 and knocking down mir-370-3p, by Transwell assay.